

The Influence of Nozzle Diameter on the Foaming Mechanism in In-Situ Foam 3D Printing

Márton Tomin¹, Viktória Kunsági¹, Péter Széplaki²

¹Department of Polymer Engineering, Budapest University of Technology and Economics

Abstract

In-situ foam 3D printing offers a promising route to improve interlayer adhesion in FDM parts by exploiting expansion during extrusion. This study investigates the effect of nozzle diameter on the foaming behavior, cell structure, and mechanical performance of PLA-based foamable filaments. Three nozzle diameters (0.4, 0.6, and 0.8 mm) were tested across different temperatures, and the resulting cellular structure, flexural and impact properties were evaluated. Results show that smaller nozzles promote finer cell structures due to increased shear and residence time, which also enhance mechanical performance through improved adhesion between deposited layer.

Introduction

3D printing is gaining increasing popularity due to the wide design freedom, rapid prototyping capabilities, and the nearly waste-free and energy-efficient manufacturing process it offers. As a result, the global additive manufacturing industry has been expanding rapidly [1]. Among the various additive manufacturing technologies, fused deposition modeling (FDM) – also referred to as fused filament fabrication (FFF) – remains the most widely used method, both in industrial and consumer applications. This technique builds parts layer by layer by extruding a molten thermoplastic material through a heated nozzle [2, 3].

According to recent market analyses, the number of FDM 3D printers sold globally continues to grow each year with an estimated compound annual growth rate (CAGR) of 21.8%, and millions of desktop units are in use worldwide, driven by both hobbyist and professional users [4]. However, the wider application of this technology for engineering purposes is still limited by the anisotropic mechanical properties of the printed parts. One of the primary issues is the weak adhesion between adjacent layers, which significantly reduces the overall mechanical performance of the printed objects [5, 6].

A promising strategy to overcome this limitation is the development of in-situ foamable filaments [7]. These materials typically consist a chemical blowing agent (CBA) [8] or thermally expandable microspheres (TEM) [9], which produce gas during the printing process in response to heat. As the polymer exits the nozzle, the pressure drop

and thermal activation trigger the foaming process. The resulting volumetric expansion can increase the contact pressure between layers, thereby enhancing interlayer bonding and improving the mechanical performance of the printed parts.

Previous studies [10-13] have extensively investigated the effects of printing temperature and speed on the foaming behavior and resulting cellular structure of printed components. However, despite its direct influence on pressure drop, shear rate, and residence time, the effect of nozzle diameter on the foaming mechanism has not yet been systematically explored.

This study aims to examine how nozzle diameter influences the foaming behavior and structural characteristics of in-situ foam 3D-printed parts. By comparing samples produced with different nozzle sizes, the relationship between process conditions, cellular morphology, and mechanical properties was assessed. Special attention was given to how changes in expansion affect interlayer adhesion and the overall performance of the printed structures

Materials

A commercially available in-situ foamable filament was used for specimen fabrication. The material, sold under the name LW-PLA (ColorFabb B.V., Belfeld, Netherlands), is based on polylactic acid (PLA) and contains an endothermic chemical blowing agent [10] that induces foaming during the extrusion process. The filament has a nominal diameter of 1.75 mm.

Methods

3D-printing

All samples were produced using a Craftbot Plus desktop FDM printer (CraftUnique Ltd., Budapest, Hungary), equipped with MK8-type hardened steel nozzles of three different diameters: 0.4 mm, 0.6 mm, and 0.8 mm.

Two experimental series were conducted. In the first, the effect of nozzle diameter on foaming characteristics was investigated at a fixed printing speed of 15 mm/s and a flow rate of 100%. Hollow cube structures with dimensions of 25 × 25 × 25 mm were printed, each surrounded by a

2 mm-wide brim to improve bed adhesion. The wall thickness of the cubes was designed to be one extrusion width, meaning each wall consisted of a single printed line per layer. This ensured that expansion occurred without constraint from adjacent extruded lines or previously deposited layers. For each nozzle size, the layer height and extrusion width were set proportionally (0.2/0.4 mm for the 0.4 mm nozzle, 0.3/0.6 mm for the 0.6 mm nozzle, and 0.4/0.8 mm for the 0.8 mm nozzle).

To examine the relationship between nozzle geometry and foaming efficiency, printing was carried out at four different temperatures: 220, 230, 240, and 250 °C. As nozzle diameter directly affects shear rate, internal pressure, and residence time, these parameters were estimated based on the methodology described in [14].

In the second experimental series, rectangular specimens (80 × 10 × 4 mm) were printed for mechanical testing at 230 °C and 15 mm/s using an extrusion multiplier of 0.8 (80% flow rate) to compensate for material expansion. The same three nozzle diameters and corresponding layer settings as in the first series were applied.

Evaluation of Foaming Efficiency

The foaming behavior of the printed samples was evaluated by scanning electron microscopy (SEM) using a JEOL JSM-6380LA device (Jeol Ltd., Tokyo, Japan). Samples were fractured in liquid nitrogen to obtain cross-sections, then sputter-coated with a thin gold-palladium layer to ensure surface conductivity.

From the SEM images, cell density (1) were calculated. In addition, average cell size was determined by image processing.

$$N_C = \left(\frac{n}{A}\right)^{\frac{3}{2}} \left[\frac{pcs}{cm^3}\right] \quad (1)$$

where N_C is the cell density (pcs/cm³), n is the number of cells visible in the SEM image (pcs), and A is the investigated area on the sample (cm²) [15].

Mechanical characterization

3-point bending tests

Flexural properties of the printed specimens were evaluated using a Zwick Z005 universal testing machine (Zwick GmbH, Ulm, Germany), equipped with a 5 kN load cell. The test setup included a support span of 64 mm, and the specimen dimensions were 80 × 10 × 4 mm. A preload of 1 N was applied at a speed of 20 mm/min, followed by

the main loading phase conducted at a crosshead speed of 5 mm/min.

The results were evaluated by determining the flexural strength at a deflection corresponding to 10% of the support spacing (2):

$$\sigma_{bh} = \frac{3Fl}{2bh^2} \quad (2)$$

where σ_{bh} is the flexural strength (MPa), F is the force recorded at 10% bending (N), L is the support distance (mm), b is the specimen width (mm), while h is the specimen height (mm).

To characterize the stiffness of printed specimens, the flexural modulus of elasticity (3) was also determined from the slope of the force-deflection curve between 0.05% and 0.25% of the relative deformation:

$$E_f = \frac{1}{4} \cdot \frac{L^3}{bh^3} \cdot \frac{\Delta F}{\Delta f} \quad (3)$$

where E_f (MPa) is the flexural modulus of elasticity, while $\Delta F/\Delta f$ (N/mm) is the slope of the loading curve in the defined deformation range.

Charpy impact tests

The impact resistance of the 3D-printed specimens was evaluated using a CEAST Fractovis 9350 instrumented drop-weight impact tester (Instron, Norwood, USA). Tests were conducted on unnotched rectangular specimens with dimensions of 80 × 10 × 4 mm, positioned on a 62 mm support span. The setup included a 4.5 kN piezoelectric force sensor for high-resolution force measurements. The impactor was accelerated to a velocity of 2.9 m/s, and the total impact energy was set to 15 J.

From the measurements, we calculated the impact strength (4) of the samples:

$$\alpha_c = \frac{E_{abs}}{bh} \quad (4)$$

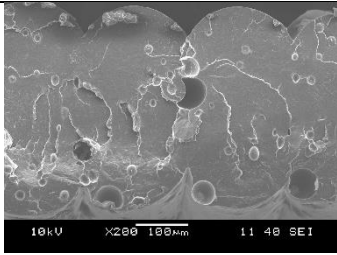
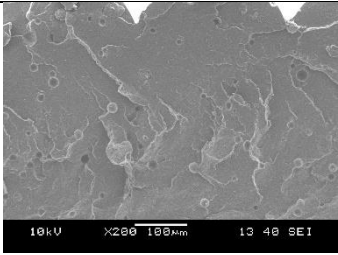
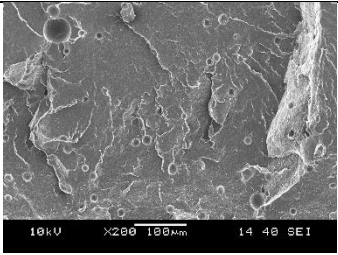
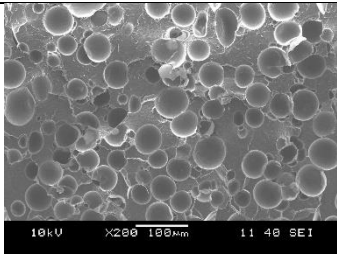
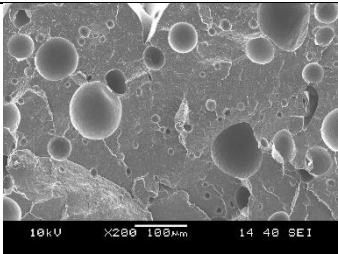
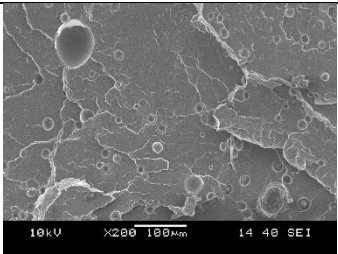
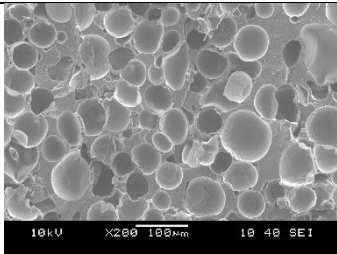
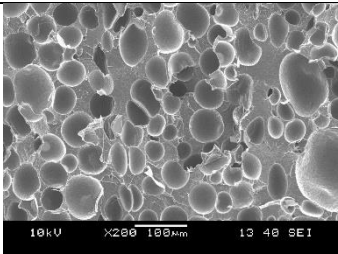
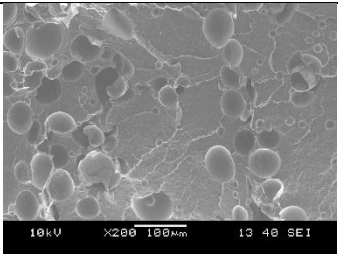
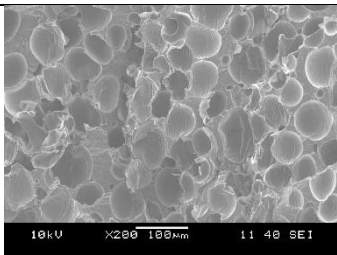
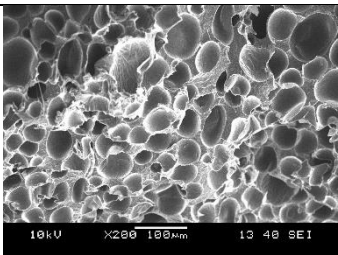
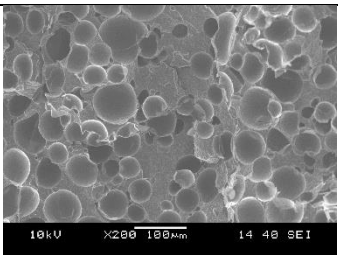
where α_c is the impact strength (kJ/m²) E_{abs} is the absorbed energy (kJ), and b and h are the specimen width and thickness (m), respectively.

Results

Evaluation of Foaming Efficiency

To visualize the effect of nozzle diameter and printing temperature on the cellular structure, SEM images were taken from the cryo-fractured surfaces of the printed hollow cubes. The images below (Table 1) illustrate how cell morphology evolves with processing parameters.

Table 1. SEM images of the structures printed at different temperatures using different nozzle diameters [14]

		Nozzle diameter [mm]		
		0.4	0.6	0.8
Printing temperature[°C]	220			
	230			
	240			
	250			

The SEM images clearly show that foaming did not occur at 220 °C, regardless of nozzle diameter. However, at 230 °C and above, significant expansion and cell formation were observed. Notably, samples printed with the smaller 0.4 mm nozzle consistently exhibited a finer, more homogeneous cellular structure across all temperatures. In contrast, larger nozzle diameters resulted in coarser and more heterogeneous cell morphology.

Although manufacturers of foamable PLA filaments typically recommend using larger nozzle diameters to prevent clogging and accommodate the material's expansion, our results indicate that smaller nozzles can actually enhance foaming efficiency. This is primarily due to the increased residence time and higher shear rate (see Figure 1 for the calculated values) associated with smaller

nozzles. Both of these factors contribute to improved thermal exposure and viscous heating, which in turn promote more complete decomposition of the blowing agent and more effective gas dissolution within the polymer melt.

Additionally, the higher internal pressure generated in smaller nozzles [16] results in a more pronounced pressure drop at the nozzle exit. This sharp drop in pressure facilitates cell nucleation and promotes subsequent cell growth, leading to a more porous structure [17].

These findings highlight that, contrary to common practice, reducing the nozzle diameter can significantly improve foaming efficiency by enhancing both the thermally induced activation of the blowing agent and the pressure-driven expansion dynamics during extrusion.

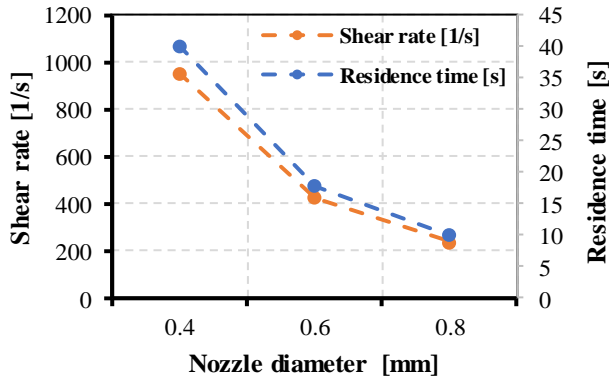


Figure 1. Calculated residence time and shear rate as a function of nozzle diameter at 15 mm/s print speed.

The quantitative evaluation of the SEM images (see Figure 2) confirmed the trends observed visually. At temperatures above 230 °C, the smallest nozzle diameter resulted in the highest cell density, indicating that increased pressure drop promoted more intensive cell nucleation. In contrast, the average cell diameter showed no clear correlation with nozzle size. Although minor differences were observed, these values remained within a similar range above 230 °C, suggesting that while nucleation was strongly affected by processing conditions, cell growth was less sensitive to the investigated parameters.

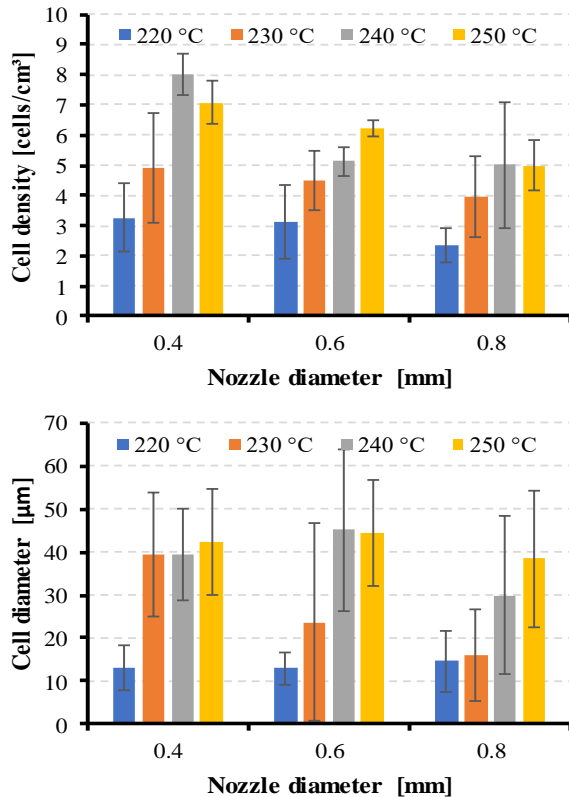


Figure 2. Cell density and cell diameter at different printing temperatures using different nozzle sizes [14].

Mechanical characterization

3-point bending tests

The results of the 3-point bending tests are presented in Figure 3. A clear trend was observed: specimens printed with smaller nozzle diameters exhibited significantly higher flexural strength and stiffness compared to those printed with larger nozzles.

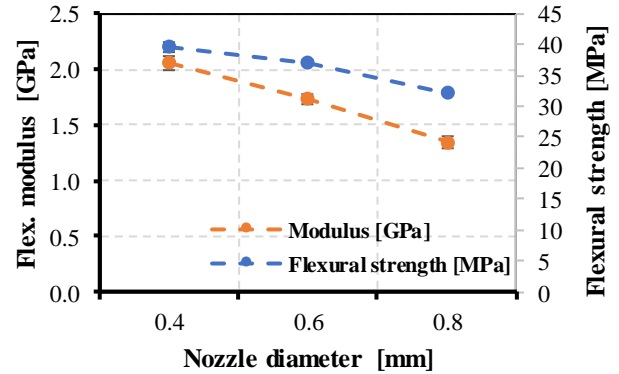


Figure 3. Flexural strength and flexural modulus of the printed specimens as a function of nozzle diameter at 230 °C.

This behavior can be primarily attributed to the differences in interlayer adhesion, which is strongly influenced by the extent of in-situ foaming. Unlike the single-wall cube samples used for foaming analysis, these mechanical test specimens consisted of multiple adjacent extruded lines. The formation of a continuous, gap-free cross-section between these lines depends on how effectively the material expands during deposition.

The lower flexural performance of specimens printed with larger nozzles suggests that foaming was less effective under these conditions, likely due to reduced residence time, lower shear rate, and a smaller pressure drop, which hindered the decomposition of the blowing agent and limited the expansion of the extrudate. As a result, visible gaps and weak interfaces remained between adjacent filaments, reducing mechanical integrity.

In contrast, samples printed with the 0.4 mm nozzle showed a much more homogeneous cellular structure, and the deposited layers expanded sufficiently to eliminate interfacial voids. This led to stronger interlayer bonding and improved load-bearing capacity under bending (see Figure 4).

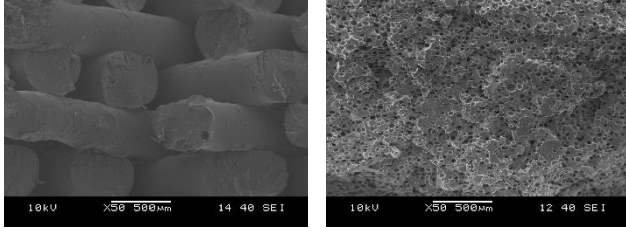


Figure 4. SEM images showing interlayer gaps without foaming (left) and improved continuity with effective foaming (right).

Charpy impact tests

The impact strength results (Figure 5) showed the same trend as in flexural tests. The highest average value was measured for the 0.4 mm nozzle (13.7 kJ/m²), followed by the 0.6 mm (11.9 kJ/m²) and 0.8 mm (11.2 kJ/m²) nozzles.

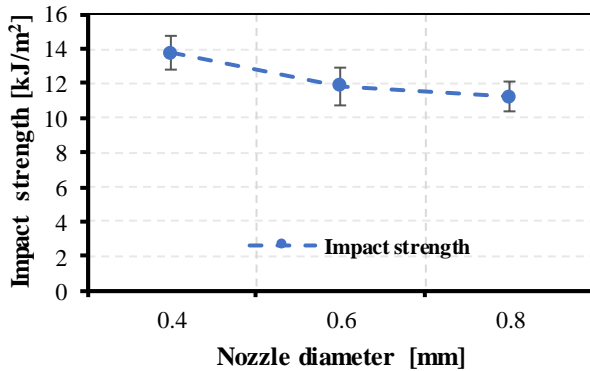


Figure 5. Impact strength of printed specimens as a function of nozzle diameter.

The differences can be linked to the extent of interlayer bonding. In samples printed with larger nozzles, the presence of gaps between layers provides an easy path for crack initiation and propagation, requiring less energy to break the specimen. In contrast, the more uniform expansion achieved with the 0.4 mm nozzle helped fill the gaps, creating a continuous structure that better resisted impact loading.

Conclusions

This study demonstrated that nozzle diameter has a significant effect on the foaming efficiency, cellular structure, and mechanical performance of in-situ foam 3D-printed PLA parts. Contrary to the general recommendations of using larger nozzles for foamable filaments, the smallest tested diameter (0.4 mm) consistently resulted in finer, more homogeneous cell morphology and superior mechanical properties.

The improved performance can be attributed to the longer residence time, higher shear rate, and greater pressure drop associated with the smaller nozzle, all of which contribute to enhanced blowing agent decomposition, gas dissolution, and cell nucleation. These effects led to more efficient expansion, which improved interlayer bonding by reducing voids between deposited layers.

Flexural and Charpy impact tests confirmed that better foaming not only reduces density but also strengthens the printed structure by promoting a more cohesive internal geometry. These findings underline the importance of carefully selecting nozzle diameter in applications where both lightweight design and mechanical performance are critical.

The obtained results can contribute to improving the mechanical strength of FDM-printed parts, or alternatively, reducing their weight without compromising mechanical performance. In the long term, these findings can be exploited in low-volume or customized applications—such as lightweight drone components or functional prototypes—where traditional mass-production methods are not economically viable.

References

1. N. Shahrubudin, T.C. Lee, and R. Ramlan, *Procedia Manufacturing*, **35**, 1286-1296 (2019).
2. D. Popescu, A. Zapciu, C. Amza, F. Baciuc, and R. Marinescu, *Polymer Testing*, **69**, 157-166 (2018).
3. I.J. Solomon, P. Sevel, and J. Gunasekaran, *Materials Today: Proceedings*, **37**, 509-514 (2021).
4. Grand View Research: Market Analysis Report, ID: GVR-4-68040-270-89.
5. A.Q. Pan, Z.F. Huang, R.J. Guo, and J. Liu, *Key Engineering Materials*, **667**, 181-186 (2016).
6. K. Kalia, B. Francoeur, A. Amirkhizi, and A. Ameli, *ACS Applied Materials & Interfaces*, **14**, 22454-22465 (2022).
7. M. Nofar, J. Utz, N. Geis, V. Altstädt, and H. Ruckdäschel, *Advanced Science*, **9**, 2105701 (2022).
8. W.J. Choi, K.S. Hwang, H.J. Kwon, C. Lee, C.H. Kim, T.H. Kim, S.W. Heo, J.-H. Kim, and J.-Y. Lee, *Materials Science and Engineering: C*, **110**, 110693 (2020).
9. Z. Nieduzak, S. Hart, Y. Joseph, K. Kalia, and A. Ameli, in *SPE FOAMS 2022*, Indianapolis, USA (2022).
10. A.R. Damanpack, A. Sousa, and M. Bodaghi, *Micromachines*, **12**, 866 (2021).
11. M. Ozdemir, and Z. Doubrovski, in *CHI Conference on Human Factors in Computing Systems*, Hamburg, Germany (2023).
12. S. Zhang, Q. Gao, Y. Zhang, X. Sheng, Z. Miao, J. Qin, G. Zhang, and X. Shi, *Additive Manufacturing*, **76**, 103770 (2023).

13. K. Kalia, A. Amirkhizi, and A. Ameli, *AIP Conference Proceedings*, **2884**, 140003 (2023).
14. V. Kunsági, P. Széplaki, and M. Tomin, *Express Polymer Letters*, **19**, 706-725 (2025).
15. M. Tomin, and Á. Kmetty, *Journal of Applied Polymer Science*, **138**, 49999 (2021).
16. S. de Vries, T. Schuller, F.J. Galindo-Rosales, and P. Fanzio, *Additive Manufacturing*, **80**, 103966 (2024).
17. C.B. Park, D.F. Baldwin, and N.P. Suh, *Polymer Engineering & Science*, **35**, 432-440 (1995).

Acknowledgments

This research was supported by the Hungarian National Research, Development and Innovation Office (K 146236). Márton Tomin is supported by the Janos Bolyai Research Scholarship of the Hungarian Academy of Sciences.